High CO_2 Chemisorption in α-Li$_5$AlO$_4$ at Low Temperatures (30−80 °C): Effect of the Water Vapor Addition
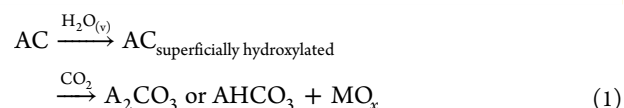
Tatiana L. Ávalos-Rendón and Heriberto Pfeiffer*

Instituto de Investigaciones en Materiales, Universidad Nacional Autónoma de México, Circuito Exterior s/n, Ciudad Universitaria, Coyoacán, CP 04510 Mexico Distrito Federal, Mexico

ABSTRACT: α-Li$_5$AlO$_4$ was synthesized using a solid-state reaction, and then different water sorption experiments were performed using N$_2$ and CO$_2$ as carrier gases. When the N$_2$−H$_2$O flow gas was used, α-Li$_5$AlO$_4$ showed a water vapor sorption because of two different processes: superficial hydration and hydroxylation. However, if CO$_2$ was used as the water vapor carrier gas, the α-Li$_5$AlO$_4$ carbonation process was observed at low temperatures (30−80 °C), although this reaction is only produced at high temperatures (200−700 °C) under dry conditions. In this case, the carbonation process was induced by the lithium ceramic superficial hydroxylation. The results clearly showed that α-Li$_5$AlO$_4$ is capable of chemisorbing up to 8.4 mmol of CO$_2$/g of ceramic, a considerably high capture at low temperatures compared to different materials. Finally, a kinetic analysis indicated that the CO$_2$ chemisorption in α-Li$_5$AlO$_4$ is highly favored in the presence of water vapor.

INTRODUCTION

The capture of CO$_2$, either physically or chemically, onto solid sorbents is receiving increasing attention, which has led to different materials being tested as possible captors. Some of these materials include zeolites, hydrotalcites, amines, polymeric membranes, calcium oxide, and different lithium ceramics.[1−3] These types of materials are in demand because they can be used in advanced zero-emission power generation technologies[1,4,5] and steam methane-reforming processes for enhanced hydrogen production.[6,7] In addition, all possible applications of the CO$_2$ capture process would help to mitigate the impact of the greenhouse effect. For this reason, different lithium ceramics have been tested for use as possible CO$_2$ captors through a chemisorption process.[8−26] Among these ceramics, lithium aluminate (α-Li$_5$AlO$_4$) appears to be one of the best options because of its high theoretical chemisorption capacity (15.9 mmol of CO$_2$/g of ceramic).[16,26−28] Note that Li$_5$AlO$_4$ is capable of chemisorbing CO$_2$ over a wide range of temperatures (200−700 °C), irrespective of its different polymorphs.[26] However, note that the α-Li$_5$AlO$_4$ polymorph has the best experimental CO$_2$ chemisorption capacity per gram currently reported.[26]

In addition, water vapor is commonly found to coexist with CO$_2$ during post-combustion CO$_2$ capture applications. Typical power plant flue gases contain approximately 72% N$_2$, 8−12% CO$_2$, 8−10% H$_2$O, and smaller concentrations of other polluting species. Consequently, studying and understanding the capture of CO$_2$ in CO$_2$−H$_2$O systems are very important; however, there are relatively few sorption data sets available in the literature for this binary system.[29,30] Specifically, among the alkaline ceramics, as in general, there are only a few papers showing the effects of water vapor during the CO$_2$ absorption on these ceramics.[11,31−35] Most of these works mention that water vapor appears to improve the CO$_2$ chemisorption because of the superficial hydroxylation, which thermodynamically enhances the CO$_2$ capture according to the following reaction mechanism:[32]

$$AC \xrightarrow{\text{H}_2\text{O}_{(v)}} AC_{\text{superficially hydroxylated}}$$
$$\xrightarrow{\text{CO}_2} A_2CO_3 \text{ or } AHCO_3 + MO_x \quad (1)$$

where AC represents the alkaline ceramic, A$_2$CO$_3$ and AHCO$_3$ correspond to the alkaline carbonate and the acid alkaline carbonate, respectively, and MO$_x$ is the residual metal oxide.

Therefore, the aim of the present work is to study the CO$_2$−H$_2$O capture process on α-Li$_5$AlO$_4$, which is one of the most promising ceramic materials for the capture of CO$_2$. These experiments were performed over a moderate temperature range (30−80 °C).

EXPERIMENTAL SECTION

The α-Li$_5$AlO$_4$ polymorph was synthesized using a solid-state reaction that employs lithium oxide (Li$_2$O, Aldrich) and γ-aluminum oxide (γ-Al$_2$O$_3$, Aldrich). The powders were first mechanically mixed and pressed into pellets (2.5 tons/cm^2). The pellets were then heated at 500 °C for 24 h. Finally, the α-Li$_5$AlO$_4$ pellets were pulverized.[26] To obtain pure α-Li$_5$AlO$_4$, a 30 wt % excess of lithium was used during synthesis because of the tendency of lithium to sublimate. The formation of α-Li$_5$AlO$_4$ was confirmed by powder X-ray diffraction (XRD) (data not shown).

Dynamic and isothermal experiments were performed using a humidity-controlled thermobalance (TA Instruments, model Q5000SA) at different temperatures and relative humidities (RHs). The experiments were performed using distilled water and two different carrier gases: nitrogen (N$_2$, Praxair grade 4.8) or carbon dioxide (CO$_2$, Praxair grade 3.0). The total gas flow rate used in all of the experiments was 100 mL/min, and the RH percentages were automatically controlled by the Q5000SA instrument. Dynamic water vapor sorption/desorption experiments were performed at different temperatures (between 30 and 80 °C) while varying the RH from 0 to 80% and then from 80 to 0% at a rate of 0.5%/min. Different isothermal experiments were performed at specific temperatures and RHs for 4 h with the use of CO$_2$ as a carrier gas. Afterward, the

products (~3 mg) were characterized to identify the hydration products. The samples were analyzed using XRD and thermogravimetric analysis (TGA). A standard X-ray diffractometer (Bruker AXS, D8 Advance) equipped with a copper anode X-ray tube was used for the XRD measurements. The Joint Committee Powder Diffraction Standards (JCPDS) were used to identify α-Li_5AlO_4 and the phases of the products from the diffraction data. The TGA measurements were performed under an air atmosphere using a TA Instruments, model Q500HR thermobalance at a heating rate of 5 °C/min.

■ RESULTS AND DISCUSSION

The α-Li_5AlO_4 water sorption–desorption curves obtained using N_2 as a carrier gas are shown in Figure 1. It is clearly
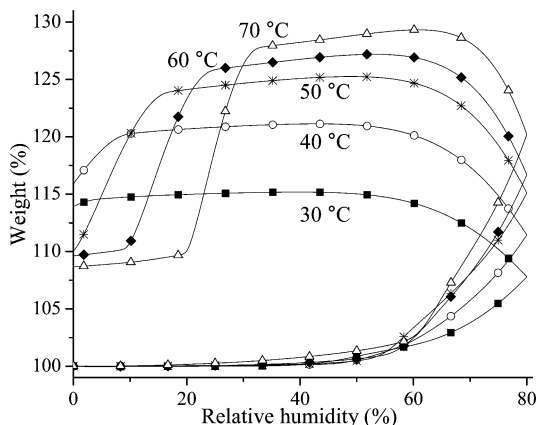

Figure 1. Water vapor isotherms of the α-Li_5AlO_4 sample, generated at temperatures between 30 and 70 °C, using N_2 as the carrier gas.

evident that all of the sorption isotherms corresponded to type III, according to the International Union of Pure and Applied Chemistry (IUPAC) classification. Additionally, the water sorption varied as a function of the temperature, and it was not completed or limited to the sorption curves, because during some part of the desorption process, the samples continued gaining weight. When the α-Li_5AlO_4 sample was treated at 30 °C, the maximum water sorption was equal to 15.1 wt %, but this quantity increased as a function of the temperature to 29.2 wt % at 70 °C. Afterward, the water desorption was proportional to the temperature, which may be attributed to water evaporation. In fact, at 30 °C, the water desorption process was almost not detected. At 40 °C, water desorption occurred at a RH of 10% and the weight loss corresponded to 5 wt %. Then, between 50 and 70 °C, the weight lost increased and this process was initiated at a higher RH. Finally, in other alkaline and earth alkaline ceramics, it has been shown that the weight gained at the end of the isothermal experiments can be attributed to H_2O that is physically and/or chemically trapped.[31−35]

Figure 2 shows the α-Li_5AlO_4 water sorption–desorption curves with the use of CO_2 as the carrier gas. Although the sorption curves were type III (as in the N_2 case), the water desorption process and the final weight increments differed. During the sorption process, the weight increments increased as a function of the temperature (see Figure 2B). In addition, note that the weight increments began increasing at approximately 20−30% RH (in the N_2 case, the weight increments began increasing at a RH higher than 50%). It appears that the flow of CO_2 produces faster and higher sorption processes. During the desorption process, the final weight increment increased between 30 and 60 °C, from 22.5
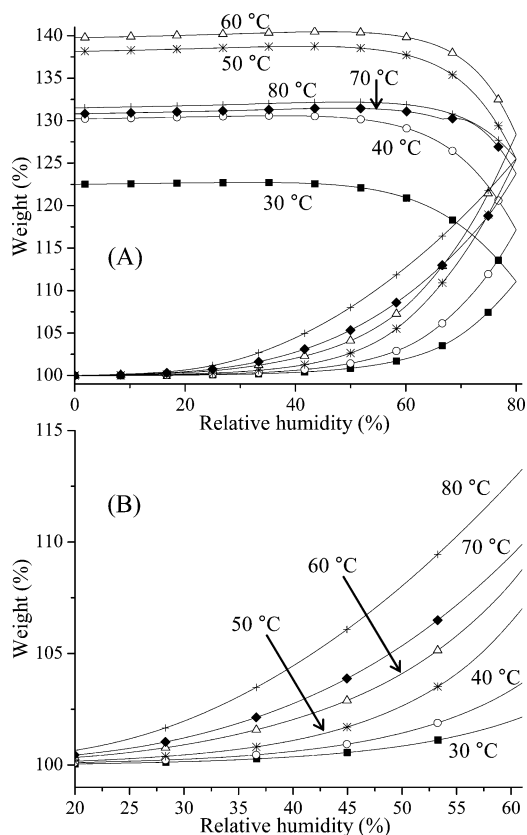

Figure 2. (A) Water vapor isotherms of the α-Li_5AlO_4 sample, generated at temperatures between 30 and 80 °C, using CO_2 as the carrier gas. (B) Initial sorptions of the same isotherms.

to 39.6 wt %. However, at $T > 60$ °C, the weight increments decreased. It appears that the CO_2−H_2O flow produced the carbonation and hydration of α-Li_5AlO_4, and the hydration may have been reduced at high temperatures because of evaporation.

To analyze the α-Li_5AlO_4/N_2−H_2O and α-Li_5AlO_4/CO_2−H_2O hydration products, some of the isothermal products were analyzed using XRD. Figure 3 shows two XRD patterns that correspond to the α-Li_5AlO_4 isothermal products treated at 60 °C in N_2−H_2O and CO_2−H_2O flows. In both cases, several new phases were detected, which provides evidence of the α-
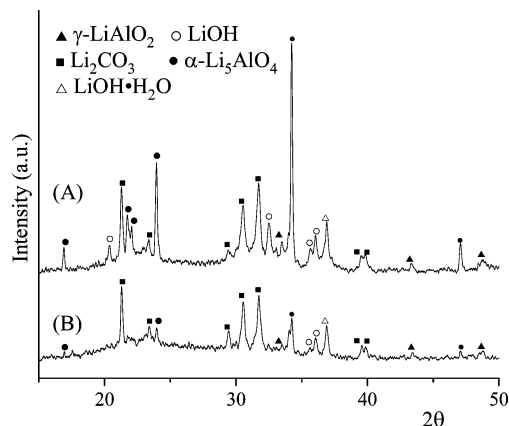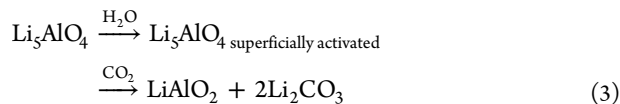

Figure 3. XRD patterns of the α-Li_5AlO_4 rehydrated samples at 60 °C, using (A) N_2 and (B) CO_2 as the carrier gases. The different phases were labeled as follows: (●) α-Li_5AlO_4, (▲) γ-$LiAlO_2$, (■) Li_2CO_3, (○) LiOH, and (△) LiOH−H_2O.

Li$_5$AlO$_4$ reactivity in both flows. When α-Li$_5$AlO$_4$ was treated in a N$_2$–H$_2$O flow, the obtained products were lithium hydroxides (LiOH and LiOH·H$_2$O), lithium carbonate (Li$_2$CO$_3$, which must be produced later because of the environmental CO$_2$), LiAlO$_2$, and Li$_5$AlO$_4$. Therefore, the reaction process occurring under these conditions on the α-Li$_5$AlO$_4$ particle surfaces is

$$\alpha\text{-Li}_5\text{AlO}_4 + 2\text{H}_2\text{O} \rightarrow \text{LiAlO}_2 + 4\text{LiOH} \qquad (2)$$
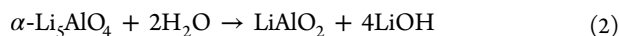
However, the XRD peak intensities suggest only a partial α-Li$_5$AlO$_4$ hydroxylation, which is in good agreement with the final weight increments observed in Figure 1.

When α-Li$_5$AlO$_4$ was treated in a CO$_2$–H$_2$O flow, the products were LiOH, LiOH·H$_2$O, Li$_2$CO$_3$, LiAlO$_2$, and α-Li$_5$AlO$_4$. However, in this case, the Li$_2$CO$_3$ phase must be produced during the isothermal experiment and the Li$_5$AlO$_4$ peak intensities decreased considerably, which suggests a much higher reaction efficiency. It has been described in the literature[26−28] that Li$_5$AlO$_4$ is able to chemisorb CO$_2$ but at $T > 200$ °C. Nevertheless, in this case, the water vapor addition allowed the CO$_2$ chemisorption to occur at much lower temperatures (30−80 °C). Perhaps the water molecules reacted with Li$_5$AlO$_4$ superficially, producing Li–OH superficial bonds. Then, superficially activated Li$_5$AlO$_4$ must be more reactive to CO$_2$. In fact, in a previous work, it was reported that LiOH is capable of chemically trapping large amounts of CO$_2$ at considerably low temperatures.[28] Therefore, α-Li$_5$AlO$_4$ may have reacted with CO$_2$ at low temperatures because of a superficial hydroxylation, according to the following reaction mechanism:

$$\text{Li}_5\text{AlO}_4 \xrightarrow{\text{H}_2\text{O}} \text{Li}_5\text{AlO}_4\text{ superficially activated}$$

$$\xrightarrow{\text{CO}_2} \text{LiAlO}_2 + 2\text{Li}_2\text{CO}_3 \qquad (3)$$

where Li$_5$AlO$_4$ superficially activated must correspond to the Li$_5$AlO$_4$ phase that was mainly hydroxylated at the surface, producing a mixture of LiAlO$_2$ and LiOH, according to reaction 2 and the different results observed by XRD.

To further understand and quantify the CO$_2$–H$_2$O reactivity on α-Li$_5$AlO$_4$, different kinetic experiments are presented in Figures 4 and 5, which correspond to the experiments performed at different temperatures and RHs with CO$_2$ flow. Figure 4 shows the isotherms performed at 80 °C while varying the RH (20, 40, 60, and 80%). As observed from the isotherms in Figure 4, the weight increased as a function of the RH. While
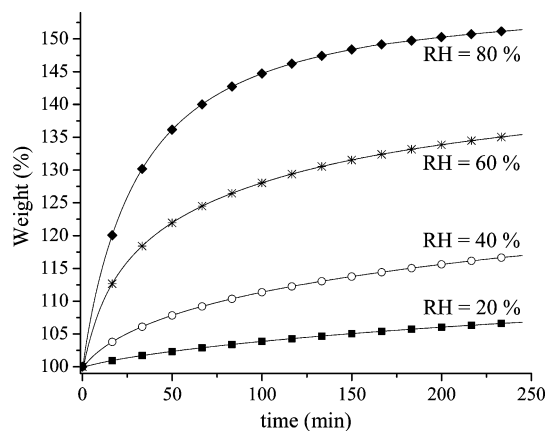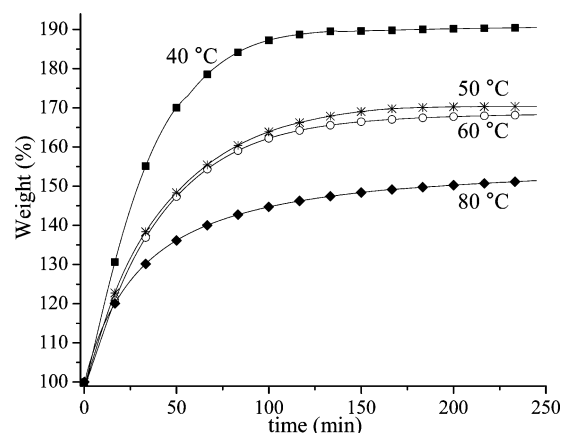
Figure 5. Kinetic isotherms performed at a RH of 80% and different temperatures (40, 50, 60, and 80 °C), using CO$_2$ as the carrier gas.

the sample analyzed with 20% RH gained 6.8 wt % after 240 min, the sample treated with 80% RH gained 51.3 wt % in the same period of time. Of course, these weight increments must be associated with different processes, such as hydration, hydroxylation, and carbonation. Additionally, during the first minutes of the curves, it can be observed that the RH significantly modifies the reaction rate processes, as the slopes of the curves varied from 0.0008 wt %/s at a RH of 20% to 1.1 wt %/s at a RH of 80%. This result indicates a 4 orders of magnitude difference.

However, when the samples are compared as a function of the temperature, the main variations were observed during the final weight increments but not at the initial rate reaction processes. For example, Figure 5 shows the samples analyzed with 80% RH at different temperatures (40, 50, 60, and 80 °C). As observed in this figure, the weight increments decreased from 90.2 to 51.5 wt % when varying the temperature from 40 to 80 °C. These results can be explained by the water evaporation process, which must be increased as a function of the temperature. Nevertheless, note that the slopes of these curves did not vary as much as in the previous case. Here, the slopes only increased from 0.01 to 0.03 wt %/s between 40 and 80 °C, respectively. Therefore, according to the isothermal curves, the CO$_2$–H$_2$O sorption process is affected more by the RH than by the temperature over this temperature range.

To quantify the carbonation and superficial hydration and/or hydroxylation on α-Li$_5$AlO$_4$, under the different thermal and humidity conditions, all of the isothermal products were characterized using TGA. As examples, Figure 6 shows the TGA and DTG curves of α-Li$_5$AlO$_4$ that was isothermally treated at 80 °C with different RHs. These thermograms show three different, well-defined temperature ranges. Initially, between room temperature and 300 °C, the samples treated at 80 and 60% of RH lost weight, which could be attributed to dehydration and some type of dehydroxylation. The dehydroxylation was proposed by a very defined peak that appeared at approximately 230 °C. The samples treated at lower RH basically did not present this process. The weight decrements in this part of the thermograms varied from 10.7 to only 1.5 wt % for the samples treated at a RH of 80 and 40%, respectively. Then, between 400 and 450 °C, the samples treated at 20, 40, and 60% of RH presented a dehydroxylation process, decreasing the weight lost as a function of the RH, which must occur because of the LiOH decomposition process. In fact, the sample treated at a RH of 80% did not show the LiOH
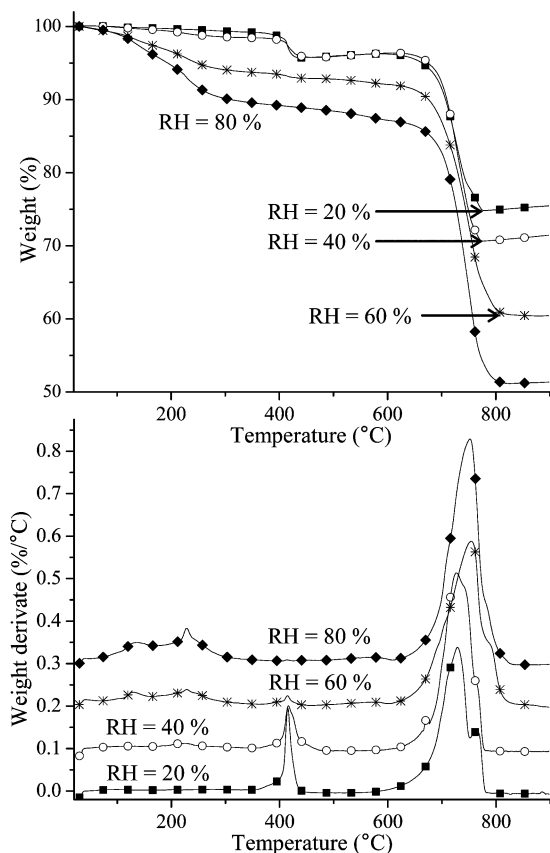
Figure 4. Kinetic isotherms performed at 80 °C and different RHs (20, 40, 60, and 80%), using CO$_2$ as the carrier gas.

Figure 6. TG and DTG curves of the α-Li$_5$AlO$_4$ rehydrated samples at 80 °C and different RHs (20, 40, 60, and 80%).

Figure 7. Evolution of CO$_2$ and H$_2$O trapped (physically and chemically) by α-Li$_5$AlO$_4$ with varying temperatures and RHs.

dehydroxylation process (400−450 °C); it only presented a superficial dehydroxylation at 230 °C. Finally, after 660 °C, all of the samples presented a decarbonation process, which appeared to increase as a function of the RH.

Therefore, to quantify the amounts of CO$_2$ and H$_2$O that were trapped (physically or chemically) by α-Li$_5$AlO$_4$, all of the weight variations that were determined from the TGA experiments were plotted in Figure 7. As observed in this figure, when the RH was fixed at 80%, the chemisorbed CO$_2$ increased as a function of the temperature, from 32.2 to 37.2 wt %. However, the trapped H$_2$O (physically and chemically) diminished as a function of the temperature because of evaporation. Moreover, when the temperature was held at 80 °C and the RH varied, the chemisorbed CO$_2$ increased, although in these cases, the H$_2$O trapped also increased, as could be expected. In this case, the CO$_2$ chemisorption was increased from 20.9 wt % with a RH of 20% to 37.2 wt % with a RH of 80%. All of these results clearly show that CO$_2$ chemisorption in α-Li$_5$AlO$_4$ is significantly improved by the presence of water in this temperature range, but in dry conditions, the capture of CO$_2$ is not achieved. This result indicates that, under the thermal humidity conditions, α-Li$_5$AlO$_4$ is capable of absorbing up to 35.8 wt % CO$_2$ (8.4 mmol of CO$_2$/g of ceramic), which corresponds to an efficiency of 53.3%. Therefore, the CO$_2$ chemisorption on α-Li$_5$AlO$_4$ under these thermal and humidity conditions is almost identical to that obtained at high temperatures and dry conditions (9.4 mmol of CO$_2$/g of ceramic[26]). Additionally, α-Li$_5$AlO$_4$ in the presence of wat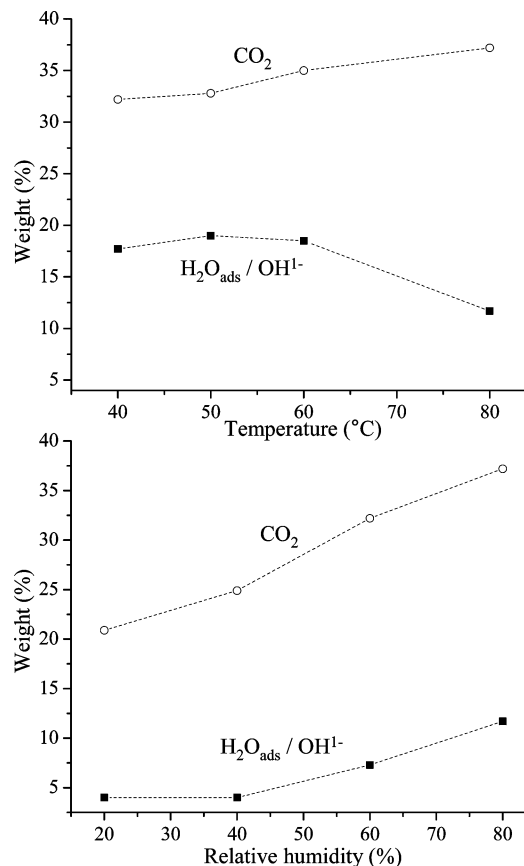er vapor appears to be capable of chemically trapping more CO$_2$ than any other material at low temperatures (30−80 °C), including activated carbons, zeolites, and amines.[1]

■ CONCLUSION

The CO$_2$−H$_2$O sorption process of α-Li$_5$AlO$_4$ was evaluated at low temperatures (30−80 °C). The initial results obtained using N$_2$ as the carrier gas showed that α-Li$_5$AlO$_4$ is capable of partially trapping water physically and chemically. In the second case, a α-Li$_5$AlO$_4$ surface hydroxylation is formed and the quantities of physically and chemically trapped water vapor were dependent upon the temperature and RH.

When CO$_2$ was used as the H$_2$O vapor carrier gas, important changes appeared in the results. Although α-Li$_5$AlO$_4$ continued trapping H$_2$O by the same mechanisms, CO$_2$ was chemically trapped as well, which produced Li$_2$CO$_3$ and LiAlO$_2$. In fact, different isothermal analyses and the characterization of the isothermal products showed that the formation of Li$_2$CO$_3$ increased as a function of the temperature but mainly as a function of the RH. Finally, note that α-Li$_5$AlO$_4$ presents considerably better CO$_2$ chemisorption efficiencies in the presence of water vapor (at low temperatures) because of the initial hydroxylation of the ceramic surface, thus promoting a higher CO$_2$ reactivity of the newly activated surfaces. In fact, α-Li$_5$AlO$_4$ is not capable of trapping CO$_2$ in the same temperature range under dry conditions.

In summary, α-Li$_5$AlO$_4$ appears to possess excellent properties for use as a CO$_2$ captor at high and low temperatures. In fact, at high temperatures, α-Li$_5$AlO$_4$ has similar capture efficiencies to CaO, which is one of the most promising and studied CO$_2$ captors at high temperatures.

Moreover, at low temperatures (30−80 °C) and in the presence of water vapor, α-Li$_5$AlO$_4$ appears to be capable of capturing more CO_2 than any other material currently reported.

■ AUTHOR INFORMATION

Corresponding Author

*Telephone: +52-55-5622-4627. Fax: +52-55-5616-1371. E-mail: pfeiffer@iim.unam.mx.

Notes

The authors declare no competing financial interest.

■ REFERENCES

(1) Choi, S.; Drese, J. H.; Jones, C. W. Adsorbent materials for carbon dioxide capture from large anthropogenic point sources. *ChemSusChem* **2009**, *2*, 796.

(2) Wang, Q.; Luo, J.; Zhong, Z.; Borgna, A. CO_2 capture by solid adsorbents and their applications: Current status and new trends. *Energy Environ. Sci.* **2011**, *4*, 42.

(3) *Advances in CO_2 Conversion and Utilization*; Yun-Hang, H., Ed.; American Chemical Society (ACS): Washington, D.C., 2010; ACS Symposium Series, Vol. *1056*.

(4) Liu, W.; Feng, B.; Wu, Y.; Wang, G.; Barry, J.; da Costa, J. C. D. Synthesis of sintering-resistant sorbents for CO_2 capture. *Environ. Sci. Technol.* **2010**, *44*, 3093.

(5) Lackner, K. S. A guide to CO_2 sequestration. *Science* **2003**, *300*, 1677.

(6) Halabi, M. H.; de Croon, M. H. J. M.; van der Schaaf, J.; Cobden, P. D.; Schouten, J. C. Reactor modeling of sorption-enhanced autothermal reforming of methane. Part I: Performance study of hydrotalcite and lithium zirconate-based processes. *Chem. Eng. J.* **2011**, *168*, 872.

(7) Waldron, W. F.; Hufton, J. R.; Sircar, S. Production of hydrogen by cyclic sorption enhanced reaction process. *AIChE J.* **2001**, *47*, 1477.

(8) Olivares-Marín, M.; Castro-Díaz, M.; Drage, T. C.; Maroto-Valerand, M. M. Use of small-amplitude oscillatory shear rheometry to study the flow properties of pure and potassium-doped Li$_2$ZrO$_3$ sorbents during the sorption of CO_2 at high temperatures. *Sep. Purif. Technol.* **2010**, *73*, 415.

(9) Pfeiffer, H.; Bosch, P. Thermal stability and high-temperature carbon dioxide sorption on hexa-lithium zirconate (Li$_6$Zr$_2$O$_7$). *Chem. Mater.* **2005**, *17*, 1704.

(10) Duan, Y. Electronic structural and electrochemical properties of lithium zirconates and their capabilities of CO_2 capture: A first-principles density-functional theory and phonon dynamics approach. *J. Renewable Sustainable Energy* **2011**, *3*, 013102.

(11) Nair, B. N.; Burwood, R. P.; Goh, V. J.; Nakagawa, K.; Yamaguchi, T. Lithium based ceramic materials and membranes for high temperature CO_2 separation. *Prog. Mater. Sci.* **2009**, *54*, 511.

(12) Wang, K.; Guo, X.; Zhao, P.; Wang, F.; Zheng, C. High temperature capture of CO_2 on lithium-based sorbents from rice husk ash. *J. Hazard. Mater.* **2011**, *189*, 307.

(13) Rodríguez-Mosqueda, R.; Pfeiffer, H. Thermokinetic analysis of the CO_2 chemisorption on Li$_4$SiO$_4$ by using different gas flow rates and particle sizes. *J. Phys. Chem. A* **2010**, *114*, 4535.

(14) Yamaguchi, T.; Niitsuma, T.; Nair, B. N.; Nakagawa, K. Lithium silicate based membranes for high temperature CO_2 separation. *J. Membr. Sci.* **2007**, *294*, 16.

(15) Khokhani, M.; Khomane, R. B.; Kulkarni, B. D. Sodium-doped lithium zirconate nano-squares: Synthesis, characterization and applications for CO_2 sequestration. *J. Sol-Gel Sci. Technol.* **2012**, *61*, 316.

(16) Ávalos-Rendón, T.; Casa-Madrid, J.; Pfeiffer, H. Thermochemical capture of carbon dioxide on lithium aluminates (LiAlO$_2$ and Li$_5$AlO$_4$): A new option for the CO_2 absorption. *J. Phys. Chem. A* **2009**, *113*, 6919.

(17) Xiao, Q.; Liu, Y.; Zhong, Y.; Zhu, W. A citrate sol−gel method to synthesize Li$_2$ZrO$_3$ nanocrystals with improved CO_2 capture properties. *J. Mater. Chem.* **2011**, *21*, 3838.

(18) Yin, X. S.; Li, S. P.; Zhang, Q. H.; Yu, J. G. Synthesis and CO_2 adsorption characteristics of lithium zirconates, with high lithia content. *J. Am. Ceram. Soc.* **2010**, *93*, 2837.

(19) Iwan, A.; Stephenson, H.; Ketchie, W. C.; Lapkin, A. A. High temperature sequestration of CO_2 using lithium zirconates. *Chem. Eng. J.* **2009**, *146*, 249.

(20) Yin, X. S.; Li, S. P.; Zhang, Q. H.; Yu, J. G. High-temperature CO_2 capture on Li$_6$Zr$_2$O$_7$: Experimental and modeling studies. *Ind. Eng. Chem. Res.* **2010**, *49*, 6593.

(21) Olivares-Marín, M.; Drage, T. C.; Maroto-Valer, M. M. Novel lithium-based sorbents from fly ashes for CO_2 capture at high temperatures. *Int. J. Greenhouse Gas Control* **2010**, *4*, 623.

(22) Seggiani, M.; Puccini, M.; S. Vitolo, S. High-temperature and low concentration CO_2 sorption on Li$_4$SiO$_4$ based sorbents: Study of the used silica and doping method effects. *Int. J. Greenhouse Gas Control* **2011**, *5*, 741.

(23) Yin, X. S.; Zhang, Q. H.; Yu, J. G. Three-step calcination synthesis of high-purity Li$_8$ZrO$_6$ with CO_2 absorption properties. *Inorg. Chem.* **2011**, *7*, 2844.

(24) Radfarnia, H. R.; Iliuta, M. C. Surfactant-template/ultrasound-assisted method for the preparation of porous nanoparticle lithium zirconate. *Ind. Eng. Chem. Res.* **2011**, *50*, 9295.

(25) Xiao, Q.; Tang, X.; Liu, Y.; Zhong, Y.; Zhu, W. Citrate route to prepare K-doped Li$_2$ZrO$_3$ sorbents with excellent CO_2 capture properties. *Chem. Eng. J.* **2011**, *174*, 231.

(26) Ávalos-Rendón, T.; Lara, V. H.; Pfeiffer, H. CO_2 chemisorption and cyclability analyses of lithium aluminate polymorphs (α- and β-Li$_5$AlO$_4$). *Ind. Eng. Chem. Res.* **2012**, *51*, 2622.

(27) Korake, P. V.; Gaikwad, A. G. Capture of carbon dioxide over porous solid adsorbents lithium silicate, lithium aluminate and magnesium aluminate at pre-combustion temperatures. *Front. Chem. Eng. China* **2011**, *5*, 215.

(28) Inoue, R.; Ueda, S.; Wakuta, K.; Sasaki, S.; Ariyama, T. Thermodynamic consideration on the absorption properties of carbon dioxide to basic oxide. *ISIJ Int.* **2010**, *50*, 1532.

(29) Li, G.; Xiao, P.; Webley, P.; Zhang, J.; Singh, R. Capture of CO_2 from high humidity flue gas by vacuum swing adsorption with zeolite 13X. *Adsorption* **2008**, *14*, 415.

(30) Li, G.; Xiao, P.; Webley, P. Binary adsorption equilibrium of carbon dioxide and water vapor on activated alumina. *Langmuir* **2009**, *25*, 10666.

(31) Ochoa-Fernandez, E.; Zhao, T.; Ronning, M.; Chen, D. Effects of steam addition on the properties of high temperature ceramic CO_2 acceptors. *J. Environ. Eng.* **2009**, *37*, 397.

(32) Santillan-Reyes, G. G.; Pfeiffer, H. Analysis of the CO_2 capture in sodium zirconate (Na$_2$ZrO$_3$). Effect of the water vapor addition. *Int. J. Greenhouse Gas Control* **2011**, *5*, 1624.

(33) Martínez-dlCruz, L.; Pfeiffer, H. Towards understanding the effect of water sorption on lithium zirconate (Li$_2$ZrO$_3$) during its carbonation process at low temperatures. *J. Phys. Chem. C* **2010**, *114*, 9453.

(34) Ortiz-Landeros, J.; Martínez-dlCruz, L.; Gómez-Yáñez, C.; Pfeiffer, H. Towards understanding the thermoanalysis of water sorption on lithium orthosilicate (Li$_4$SiO$_4$). *Thermochim. Acta* **2011**, *515*, 73.

(35) Ortiz-Landeros, J.; Gómez-Yáñez, C.; Pfeiffer, H. Surfactant-assisted hydrothermal crystallization of nanostructured lithium metasilicate (Li$_2$SiO$_3$) hollow spheres: II) Textural analysis and CO_2−H_2O sorption evaluation. *J. Solid State Chem.* **2011**, *184*, 2257.